



Article

Adsorption of Polycyclic Aromatic Hydrocarbons by Natural, Synthetic and Modified Clays

Sara Satouh ¹, Julia Martín ^{2,*} , María del Mar Orta ³, Santiago Medina-Carrasco ⁴ , Nabil Messikh ⁵, Nabil Bougdah ^{1,5}, Juan Luis Santos ² , Irene Aparicio ² and Esteban Alonso ²

- ¹ Laboratory LRPCSI, University 20 August 1955, Skikda 21000, Algeria; satouhsara14@gmail.com (S.S.); bougdah_nabil@yahoo.fr (N.B.)
- ² Departamento de Química Analítica, Escuela Politécnica Superior, Universidad de Sevilla, C/Virgen de África 7, 41011 Sevilla, Spain; jlsantos@us.es (J.L.S.); iaparcio@us.es (I.A.); ealonso@us.es (E.A.)
- ³ Departamento de Química Analítica, Facultad de Farmacia, Universidad de Sevilla, C/Profesor García González 2, 41012 Sevilla, Spain; enmaorta@us.es
- ⁴ Laboratorio de Rayos-X (CITIUS), Universidad de Sevilla, Avenida Reina Mercedes 4B, 41012 Sevilla, Spain; sanmedi@us.es
- ⁵ Department of Petrochemistry and Process Engineering, Faculty of Technology, University 20 August 1955, Skikda 21000, Algeria; nbchem@yahoo.com
- * Correspondence: jbueno@us.es

Abstract: Polycyclic aromatic hydrocarbons (PAHs) are of major scientific concern owing to their widespread presence in environmental compartments and their potential toxicological effects on humans and biota. In this study, the adsorption capacity of natural (montmorillonite (Mt)), synthetic (Na-Mica-4), and modified (with octadecylamine and octadecyltrimethylamine (ODA-Mt, ODA-Mica-4, and ODTMA-Mt and ODTMA-Mica-4)) clays were assessed and compared for the removal of 16 PAHs. Materials were synthesized and characterized by X-Ray diffraction, Zeta potential, and Fourier-transform infrared spectroscopy. The results showed its correct preparation and the incorporation of PAHs in the structure of the clays after the adsorption tests. The proposed materials were effective PAH adsorbents, with adsorption percentages close to 100%, in particular those using Mt. Mt and Na-Mica-4 presented a better adsorption capacity than their organofunctionalized derivatives, indicating that the adsorption of PAHs may occur both in the surface part and in the interlayer. The proposed adsorbents take the advantage of being a low cost and highly effective. They can be an interesting alternative for wastewater treatment and soil remediation to prevent PAH contamination.

Keywords: montmorillonite; Na-Mica-4; modified clays; persistent organic pollutants; environmental samples



Citation: Satouh, S.; Martín, J.; Orta, M.d.M.; Medina-Carrasco, S.; Messikh, N.; Bougdah, N.; Santos, J.L.; Aparicio, I.; Alonso, E. Adsorption of Polycyclic Aromatic Hydrocarbons by Natural, Synthetic and Modified Clays. *Environments* **2021**, *8*, 124. <https://doi.org/10.3390/environments8110124>

Academic Editor: Paula Alvarenga

Received: 14 October 2021

Accepted: 12 November 2021

Published: 16 November 2021

Publisher's Note: MDPI stays neutral with regard to jurisdictional claims in published maps and institutional affiliations.



Copyright: © 2021 by the authors. Licensee MDPI, Basel, Switzerland. This article is an open access article distributed under the terms and conditions of the Creative Commons Attribution (CC BY) license (<https://creativecommons.org/licenses/by/4.0/>).

1. Introduction

Polycyclic aromatic hydrocarbons (PAHs) are priority pollutants formed from the incomplete combustion of organic matter such as wood, coal, oil and fossil fuels such as diesel and petrol, among others. PAHs can be released into the environment via wastewater discharges, landfill leachate, accidental discharge or atmospheric deposition [1]. PAHs are ubiquitous and widely distributed in all the environmental compartments (water bodies [2], soil and sediments [3,4], air [5] or biota [6]), even in remote regions. Those found at a higher concentration are fluoranthene (Flt), phenanthrene (Phen), pyrene (Pyr), and anthracene (Ant). Although more than 100 PAHs have been identified, only 16 are classified as priority pollutants by the US EPA and EU due to their mutagenic, potentially carcinogenic, and highly toxic nature [7]. PAHs disrupt the DNA structure of the body, cause various types of cancer and suppress the immune system [6–9].

It is well-known that PAH compounds are not clearly removed when the traditional physicochemical methods are applied and as consequence it has resulted in the search of other types of PAH removal methods [10,11] such as adsorption [12], chemical oxidation [13], or bioremediation [14]. Considering its operational simplicity and low cost for maintenance the adsorption method is one of the best alternatives [15–17]. Activated carbon is the most widely used conventional adsorbent, but its high cost and difficult regeneration are clear disadvantages [15]. Other adsorbents such as zeolites, organic waste products, clays or silica have been proposed to successfully remove PAHs [16].

Natural clays have received much attention as adsorbents [17] due to their excellent physicochemical properties (ion exchange capacities, swelling behavior, and surface area), availability and the absence of secondary by-products [18,19]. Clays such as bentonite, sepiolite, montmorillonite (Mt) or zeolite have been widely used to remove Phen, Pyr and benzo(a)pyrene (BaP) through the adsorption process [16,18–20]. González-Santamaria et al. [20] used two natural clays (stevensite and sepiolite) to adsorb Phen from water samples. The results showed a higher adsorption capacity for stevensite because of the hydrophobic interactions and accommodation in the external planar surfaces of quasicrystals. In another attempt Sabah et al. [15] explored the potential of sepiolite to adsorb Pyr from an aqueous solution. The sepiolite surface showed a high affinity for Pyr dominated by the structural channels and the large number of Si-OH groups located on the basal surfaces.

Furthermore, clay minerals can be modified for targeting a particular contaminant. For example, the organofunctionalization of their surface allows a successful sorption of hydrophobic contaminants in the interface [21–23]. Recently, Orta et al. and Martín et al. [24,25] assessed the adsorbent capacity of two novel synthetic clays, a high-charge swelling mica (Na-Mica-4) and its organofunctionalized derivative with octadecylammonium cations (ODA-Mica-4), for the removal of several groups of emerging pollutants (surfactants, perfluoroalkyl compounds, parabens, and pharmaceuticals) from wastewater, surface water, and drinking water samples. Their results revealed a high adsorption affinity capacity (between 70 and 100%) of ODA-Mica-4 for most of the pollutants studied. The study also established a significant correlation between the log Kow of the selected pollutants and the adsorption onto the material. With specific reference to PAHs, several studies have measured its adsorption from aqueous samples. For example, employing organo-zeolite can remove 98% of fluorene (Fluo), Flt, Pyr, Phen, and benzo(a)anthracene (BaA) [18]. Recently, Dai et al. [26] synthesized a nanocomposite using organic Mt with sodium alginate and resulted an effective material for the removal of three PAHs from an aqueous solution. This material has the advantage of being recyclable and biodegradable.

Another approach is the use of clays to reduce the bioavailability of PAHs from solid environmental samples such as in soils and sediments [27,28]. PAHs are released into the atmosphere and enter the water, soil, or sediment through wet and dry deposition processes. To check the leaching of the PAH compounds from contaminated soils and sediments various remediation approaches have been adopted such as capping, stabilization and solidification, and dredging and excavation [29]. Capping immobilizes and reduces the discharge of pollutants into the natural environment and is well-thought to be an economical physical remediation method [27–30]. The in-situ capping technique with adsorbents is a frequently used engineering measure to treat sediment and soil contamination. In this sense, a variety of adsorbents including active carbon, zeolites, biochar, or clays have shown good effects in laboratory experiments [27–30]. For example, Samuelsson et al. [30] exposed two organisms to nine PAHs in the uncapped sediment to determine their bioaccumulation. Authors observed that activated carbon blended in clay showed higher contaminant retention of PAHs and less negative effects on biota than activated carbon in its pure form.

Overall, the adsorption capacity and selectivity of clays and modified clays is largely affected by the clay morphology, modification technique, the presence of exchangeable cations, and the ambient conditions (pH, temperature, ionic strength, or pollutant concentration). In this study, the adsorption capacity of natural (Mt), synthetic (Na-Mica-4), and modified (with octadecylamine and octadecyltrimethylamine (ODA-Mt, 18 ODA-Mica-4, and ODTMA-Mt and ODTMA-Mica-4)) clays for the removal of 16 PAHs was evaluated. The materials were prepared, characterized by X-Ray diffraction (XRD), Zeta potential, and Fourier-transform infrared spectroscopy (FT-IR) and subjected to adsorption tests. To the best of our knowledge, this is the first time that the six selected clays have been examined and compared as adsorbents of a high number of PAHs (16). Mt has attracted great interest because of its high cation exchange capacity (CEC), large specific surface area, low price, easy availability, and good biocompatibility. The synthetic highly charged mica, Na-mica-4, exhibits an unusual swelling behavior and selective cation exchange properties, which may become potentially useful for hazardous cation separations from solutions.

2. Materials and Methods

2.1. Reagents

A standard mixture of 16 PAHs (EPA 8270 PAH mix 3) containing naphthalene (Naph, 1000 mg/L), acenaphthylene (Acy, 2000 mg/L), acenaphthene (Ace, 1000 mg/L), fluorene (Fluo, 100 mg/L), phenanthrene (Phen, 100 mg/L), anthracene (Ant, 100 mg/L), fluoranthene (Flt, 100 mg/L), pyrene (Pyr, 100 mg/L), benzo(a)anthracene (BaA, 100 mg/L), chrysene (Chry, 100 mg/L), benzo(b)fluoranthene (BbF, 100 mg/L), benzo(k)fluoranthene (BkF, 100 mg/L), benzo(a)pyrene (BaP, 100 mg/L), dibenzo(a,h)anthracene (DahA, 200 mg/L), benzo(g,h,i)perylene (BghiP, 100 mg/L), and indeno(1,2,3-cd)pyrene (IcdP, 100 mg/L) was purchased from Sigma-Aldrich (Steinheim, Germany). The molecular structure and physicochemical properties of the PAHs are recompiled in Table 1 [31]. The PAH stock solution was prepared in acetonitrile and stored at 4 °C. Working solutions were prepared by dilution of the stock standard solution in water.

SiO₂, Al(OH)₃, MgF₂, NaCl, HCl, ODA, and ODTMA salt were purchased from Sigma-Aldrich. All of them were of analytical grade.

HPLC-grade acetonitrile and water were supplied by Romil Ltd. (Barcelona, Spain).

Table 1. Molecular structure and physicochemical properties of the PAHs.

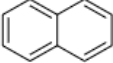
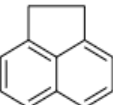
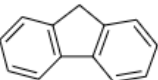
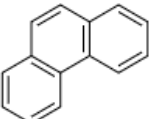
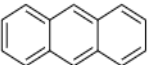
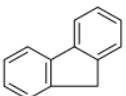
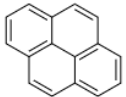
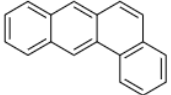
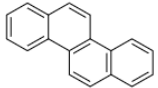
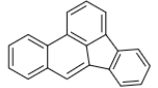
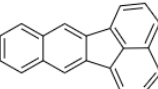
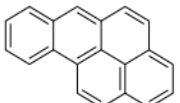
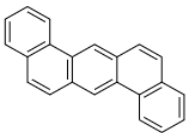
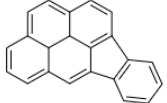
| PAH | Molecular Structure | Molecular Weight (g/mol) | Solubility in Water at 25 °C (µg/L) | Melting-Point (°C) | Boiling-Point (°C) | Vapor Pressure (Pa at 25 °C) | Log K _{ow} |
|--------------------|---|--------------------------|-------------------------------------|--------------------|--------------------|------------------------------|---------------------|
| Naphthalene |  | 128.2 | 3.17×10^4 | 81 | 217.9 | 10.4 | 3.4 |
| Acenaphthene |  | 154.2 | 3.93×10^3 | 95 | 279 | 2.9×10^{-1} | 3.92 |
| Fluorene |  | 166.2 | 1.98×10^3 | 115–116 | 295 | 8.0×10^{-2} | 4.18 |
| Phenanthrene |  | 178.2 | 1.29×10^3 | 100.5 | 340 | 1.6×10^{-2} | 4.6 |
| Anthracene |  | 178.2 | 73 | 216.4 | 342 | 8.0×10^{-4} | 4.5 |
| Fluoranthene |  | 202.3 | 260 | 108.8 | 375 | 1.2×10^{-3} | 5.22 |
| Pyrene |  | 203.3 | 135 | 150.4 | 393 | 6.0×10^{-4} | 5.18 |
| Benzo(a)anthracene |  | 228.3 | 14 | 160.7 | 400 | 2.8×10^{-5} | 5.61 |

Table 1. Cont.

| PAH | Molecular Structure | Molecular Weight (g/mol) | Solubility in Water at 25 °C (µg/L) | Melting-Point (°C) | Boiling-Point (°C) | Vapor Pressure (Pa at 25 °C) | Log K _{ow} |
|------------------------|---|--------------------------|-------------------------------------|--------------------|--------------------|---------------------------------|---------------------|
| Chrysene |  | 228.3 | 2.0 | 253.8 | 448 | 8.4×10^{-5} (20 °C) | 5.9 |
| Benzo(b)fluoranthene |  | 252.3 | 1.2 (20 °C) | 168.3 | 481 | 6.7×10^{-5} (20 °C) | 6.12 |
| Benzo(k)fluoranthene |  | 252.3 | 0.76 | 215.7 | 480 | 1.3×10^{-8} (20 °C) | 6.84 |
| Benzo(a)pyrene |  | 252.3 | 3.8 | 178.1 | 496 | 7.3×10^{-7} | 6.50 |
| Dibenzo(a,h)anthracene |  | 278.4 | 0.5 (27 °C) | 266.6 | 524 | 1.3×10^{-8} (20 °C) | 6.50 |
| Benzo(g,h,i)perylene |  | 276.3 | 0.26 | 278.3 | 545 | 1.4×10^{-8} | 7.10 |
| Indeno(1,2,3-cd)pyrene |  | 276.3 | 62 | 163.6 | 536 | 1.3×10^{-8} (20 °C) | 6.58 |

2.2. Adsorbent Materials: Description and Synthesis

Mt: Mt ($[(\text{Si}_{3.83}\text{Al}_{0.11})(\text{Al}_{1.43}\text{Fe}^{3+}_{0.26}\text{Mg}_{0.30})\text{O}_{10}(\text{OH})_2]\text{Na}_{0.30}\text{Ca}_{0.09}\text{K}_{0.01}$), naturally from Patagonia (Rio Negro, Argentina), was provided by Catiglioni Pes and Co. (Buenos Aires, Argentina). The mineral composition is Na-Mt (>99%) with quartz and feldspars as minor phases [32]. The CEC is 0.83 mequiv/g clay [33].

Na-Mica-4: The synthesis of Na-Mica-4 was carried out through the sodium chloride melt method as it was previously described by Alba et al. [34]. The starting reagents (SiO_2 , $\text{Al}(\text{OH})_3$, MgF_2 , NaCl) were weighed and mixed in an agate mortar. Subsequently, the mixture was heated at 900 °C for 15 h (rate 10 °C/min) in a platinum crucible. The solid obtained was washed with distilled water, filtrated, and dried (room temperature). Finally, the product was ground vigorously in an agate mortar. The chemical formula is $\text{Na}_4[\text{Si}_4\text{Al}_4]\text{Mg}_6\text{O}_{20}\text{F}_4 \cdot n\text{H}_2\text{O}$ and the CEC of 4.68 mequiv/g.

The organofunctionalization of Mt and Na-Mica-4 with ODA: The organoclays ODA-Mt and ODA-Mica-4 were prepared through a cation exchange reaction between the Mt/or Na-Mica-4 and an excess of ODA (2 CEC of Mt/or Na-Mica-4) [35,36]. The ODA was dissolved in an equivalent amount of HCl (0.1 M) and stirred for 3 h at 80 °C. Then, the solution was mixed with 1 g of Mt/or 2 g of Na-Mica-4 and stirred for 3 h at 80 °C. Deionized water (100 mL at 50 °C) was added to the mixture and stirred for 30 min at 50 °C. The dispersion was centrifuged at 8000 rpm for 30 min at 5 °C. Then, the solid was washed three times with deionized water. The product was dried at room temperature.

The organofunctionalization of Mt and Na-Mica-4 with ODTMA: The organoclays ODTMA-Mt and ODTMA-Mica-4 were prepared through a cation exchange reaction between the Mt/or Na-Mica-4 and an excess of ODTMA (2 CEC of Mt/or Na-Mica-4) [36]. Distilled water was added (50 mL for Mt or 300 mL for Na-Mica-4) and the solution was stirred for 3 h at 60 °C. Then, a small quantity of deionized water was added (15 mL for Mt and 50 mL for Na-Mica-4) and left in agitation (30 min at 50 °C). The dispersion was centrifuged at 8000 rpm for 30 min at 5 °C. The product was washed three times with deionized water. The product was dried at room temperature.

2.3. Characterization Methods

XRD, Z potential, and FT-IR provide useful information on the structure of clays, interlayer space, angle of inclination of the surfactants in the interlayer of organomodified clays and degree of stacking, surface charge, and the functional groups and types of bonds of the compounds. The analysis of the results before and after the adsorption assays can help us to elucidate the type of interaction between the clay and the contaminants.

2.3.1. X-ray Diffraction

XRD patterns were obtained on powder samples through a Bruker D8 Advance A25 diffractometer (Bruker, Germany) aligned in Bragg–Brentano geometry. The detector used was a Lynxeye PSD detector (Bruker, Germany), operated at 40 kV and 30 mA for copper $\text{K}\alpha$ radiation (0.15405 nm wavelength). XRD scans were performed with a 2θ range from 1° to 70°, with a step size of 0.03° (2θ) and a counting time of 0.1 s/step at the Research, Technology and Innovation Center of the University of Sevilla (CITIUS).

The diffractometer was calibrated mechanically and the corundum standard was used to check the resolution in a wide range of angles.

The Le Bail fits of the patterns were performed with the software TOPAS 6 from Bruker [37] using the fundamental parameters method. The zero error [2 θ], sample displacement, absorption, and lattice parameters of the phases were allowed to vary in order to search for the best fittings. The background was fitted by a fourth-order Chebyshev polynomial. Lorentz and polarization geometric factors for the configuration of measurement were used [38].

The angle (α) of inclination of the alkylammonium axis in the interlayer space were calculated by plotting the basal spacing (d_{001}) against the length of the alkylammonium ion chain length (n_c), using the Equation (1) [39]:

$$d_{001} = 2[(n_c - 1)0.126 + 0.131] \sin \alpha + 0.94(\text{nm}) \quad (1)$$

The average number of clay platelets stacked (N) and its modification by different functionalization were determined as in previous work [40], through Equation (2):

$$N = 1 + (D001/d001) \quad (2)$$

where the mean crystallite domain size, $D001$, was determined by the Scherrer equation on the Le Bail adjustment, and d_{001} was the basal spacing of 001 reflection of the clay layers [41].

2.3.2. Zeta Potential

The Zeta potential measurements were obtained using a Zetasizer Nanosystem system (Malvern Instruments, Southborough, MA, USA). The values were calculated using the Smoluchowski's equation [42] following the methodology described by Orta et al. [24]. The pH of the solution was measured with a Crison GLP 21 pH meter.

2.3.3. Fourier-Transform Infrared Spectroscopy

The FT-IR spectrum was collected in the range 4000–400 cm^{-1} , with a resolution of 4 cm^{-1} , after 32 scans, in a Tensor II spectrometer (Bruker, Germany). Samples were previously prepared using the KBr pellet technique. The pellets were optimized by pressing a mixture of sample and dried KBr (at 8 t cm^{-2} for 2 wt% sample concentration).

2.4. Adsorption Batch Experiments

A volume of 10 mL of a PAH mixture solution (Naph, 500 ng/mL; Acy, 1000 ng/mL; Ace, 500 ng/mL; Fluo, 50 ng/mL; Phen, 50 ng/mL; Ant, 50 ng/mL; Flt, 50 ng/mL; Pyr, 50 ng/mL; BaA, 50 ng/mL; Chry, 50 ng/mL; BbF, 50 ng/mL; BkF, 50 ng/mL; BaP, 50 ng/mL; DahA, 100 ng/mL; BghiP, 50 ng/mL; IcdP, 50 ng/mL in water) was placed into a 25 mL flask containing 10 mg of each material (Mt, Na-Mica-4, ODA-Mt, ODA-Mica-4, ODTMA-Mt and ODTMA-Mica-4). Note that the concentration levels were selected based on the concentration frequently measured for PAHs in environmental samples [43–46]. The mixture was stirred at 600 rpm for 24 h. Subsequently, the supernatants were filtered (0.45 μm nylon filter) and an aliquot of 20 μL was injected into the HPLC system. Each experiment was carried out in triplicates. The adsorption percentage of PAHs on each material was calculated as:

$$\text{Adsorption (\%)} = \frac{(C_0 - C_f)}{C_0} \times 100 \quad (3)$$

where C_0 is the concentration of PAH in the initial solution, and C_f is the concentration of PAH in the solution after the adsorption test.

2.5. PAHs Analysis

Chromatographic measurements were performed using an HPLC 1200 Series instrument (Agilent, CA, USA) equipped with an ultraviolet diode array detector (DAD) and a rapid scan fluorescence detector (Fl) connected online. For PAHs separation, a LiChrospher[®] PAH (250 mm \times 3 mm i.d., 5 μm) column (Merck, Darmstadt, Germany) protected with a LiChrospher[®] 100 RP-18 (4 mm \times 4 mm i.d., 5 μm) guard column (Merck, Darmstadt, Germany) was used.

The mobile phase was composed of an HPLC-grade water as solvent A and acetonitrile as solvent B. Chromatographic elution starts with 60% of B as the initial condition (held 3 min), at a flow rate of 1 mL/min, then a linear increase in B from 60% to 100% in 12 min (held for 5 min). The column was thermostated at 30 °C. PAHs were measured by DAD (UV signal at 254 nm) and FI (excitation and emission wavelengths shown in Table 2) detectors. The UV signal was used for Acy determination because it is not fluorescent.

Table 2. Excitation and emission wavelength applied to PAH determination and limits of detection (LODs) and quantification (LOQs) of the instrument.

| PAH | $\lambda_{ex}/\lambda_{em}$ | DAD | | FI | |
|------------|-----------------------------|-------------|-------------|-------------|-------------|
| | | LOD (ng/mL) | LOQ (ng/mL) | LOD (ng/mL) | LOQ (ng/mL) |
| Naph | 280/330 | 7.50 | 25.0 | 1.50 | 5.00 |
| Ace + Fluo | 280/330 | 33.0 | 110 | 0.03 | 11.0 |
| Phen | 246/370 | 0.60 | 2.00 | 0.12 | 0.40 |
| Ant | 250/406 | 0.30 | 1.00 | 0.06 | 0.20 |
| Flt | 280/450 | 0.75 | 2.50 | 0.15 | 0.50 |
| Pyr | 270/390 | 1.50 | 5.00 | 0.30 | 1.00 |
| BaA | 265/380 | 0.75 | 2.50 | 0.15 | 0.50 |
| Chry | 265/380 | 0.75 | 2.50 | 0.15 | 0.50 |
| BbF | 290/430 | 0.30 | 1.00 | 0.06 | 0.20 |
| BkF | 290/430 | 0.30 | 1.00 | 0.06 | 0.20 |
| BaP | 290/430 | 0.75 | 2.50 | 0.15 | 0.50 |
| DahA | 290/410 | 3.00 | 10.0 | 0.60 | 2.00 |
| BghiP | 290/410 | 1.20 | 4.00 | 0.24 | 0.80 |
| IcdP | 300/500 | 0.75 | 2.50 | 0.15 | 0.50 |

The quantification was carried out using the calibration curves prepared. The calibration curves were built by linear regression of the peak areas of the standard solutions against their concentrations. Instrumental limit of detections (LODs) and quantifications (LOQs) were calculated as the lowest observable concentration giving a signal/noise ratio of 3:1 and 10:1, respectively. A DAD and FI chromatograms of a PAH mixture are shown in Figure 1.

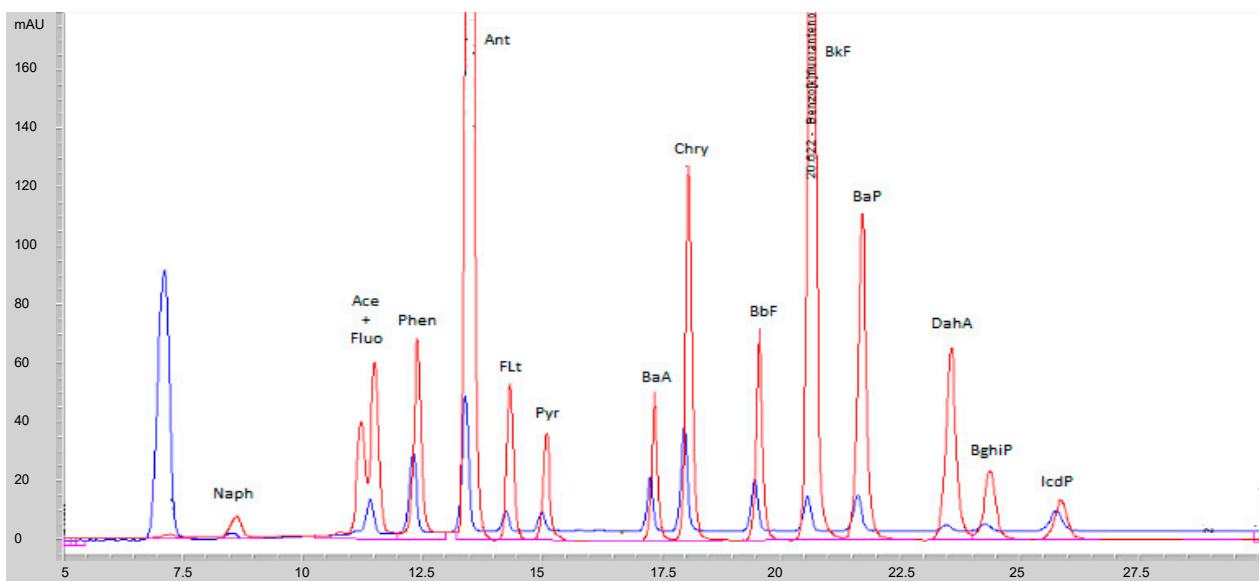


Figure 1. DAD (blue line) and FI (red line) chromatograms of a PAH mixture solution (Naph, 500 ng/mL; Acy, 1000 ng/mL; Ace, 500 ng/mL; Fluo, 50 ng/mL; Phen, 50 ng/mL; Ant, 50 ng/mL; Flt, 50 ng/mL; Pyr, 50 ng/mL; BaA, 50 ng/mL; Chry, 50 ng/mL; BbF, 50 ng/mL; BkF, 50 ng/mL; BaP, 50 ng/mL; DahA, 100 ng/mL; BghiP, 50 ng/mL; IcdP, 50 ng/mL).

3. Results

3.1. Characterization of Mt, ODA-Mt and ODTMA-Mt

3.1.1. X-ray Diffraction

The XRD Le Bail adjustment for Mt presented a GOF of 2.91 and residual factors Rwp of 12.19 and R_{Bragg} of 0.905. The structure used was Monoclinic, with C2/m Spacegroup and lattice parameters as follow: a (Å) = 5.10(15), b (Å) = 9.1(3), c (Å) = 12.7(4), beta (°) = 96.6(6). For plane (001) d (Å) = 12.66586 and 2Theta(°) = 6.97340 were obtained. For ODA-Mt the Le Bail adjustment showed a GOF of 1.99 and residual factors Rwp of 7.75 and R_{Bragg} of 0.676. The structure used was Monoclinic, with C2/m Spacegroup and lattice parameters: a (Å) = 5.016(15), b (Å) = 9.08(3), c (Å) = 22.26(6), beta (°) = 90.9(4). For plane (001) d (Å) = 22.25326 and 2Theta(°) = 3.96739 were obtained. For ODTMA-Mt the Le Bail adjustment presented a GOF of 1.25 and residual factors Rwp of 6.03 and R_{Bragg} of 0.279. The structure used was Monoclinic, with C2/m Spacegroup and lattice parameters: a (Å) = 4.836(18), b (Å) = 9.09(3), c (Å) = 21.04(7), beta (°) = 93.01(6). For plane (001) d (Å) = 21.00904 and 2Theta(°) = 4.20245 were obtained. Figure S1, in the supplementary material, shows the XRD diagrams for the 001 reflections of Mt, ODA-Mt, and ODTMA-Mt.

The angle (α) of inclination of the ODA and ODTMA axis in the interlayer space was 16.42° and 14.80°, respectively.

From the Le Bail fit, the mean crystallite domain size, d_{001} , was 7.7(3) for Mt, 3.08(5) for ODA-Mt and 11.6(3) for ODTMA-Mt. The average number of clay platelets stacked (n) calculated was 7.1 for Mt, 2.38 for ODA-Mt and 6.52 for ODTMA-Mt. The average number of platelets stacked with a high crystalline order, n, determined by Equation (2), provided an indication of the stacking order of the clay platelets [41,42], where the lower value is for ODA-Mt being the most disorderly case. This can be appreciated in Figure S1, where the ODA-Mt presents a wider peak and therefore a more disorderly stacking.

3.1.2. Zeta Potential

The external surface charge of Mt, ODA-Mt, and ODTMA-Mt was studied at pH~6.5 and the obtained values were −37.0, 49.3, and 27.2 mV for Mt, ODA-Mt and ODTMA-Mt, respectively, before adsorption assays and −36.4, 22.9, and 31.8 mV for Mt, ODA-Mt and ODTMA-Mt, respectively, after adsorption assays.

3.1.3. Fourier-Transform Infrared Spectroscopy

The vibrational spectra of Mt, ODA-Mt, and ODTMA-Mt (Figure S2) show the characteristic bands corresponding to the structural groups (OH, SiO, AlOH, AlOSi, and SiOSi) at 3632, 1040, 916, 521 and 461 cm^{-1} , respectively [35,47]. In addition, the typical bands of alkylamine described by Scheuing [48], the asymmetric and symmetrical stretching of $-\text{CH}_2$ groups at approximately 2920 and 2849 cm^{-1} of the surfactant and the bands corresponding to the bending modes in the 1750–1350 cm^{-1} can also be appreciated [35,47].

Figure 2, after adsorption assays, reveals the presence of characteristic bands of PAHs at approximately 3040, 1920, 1615, 1310, 1150, 885, 840, and 785 cm^{-1} [49,50], without significant changes in the signals of the characteristic groups of layered silicates. The bands corresponding to the PAHs were appreciated with better precision in the organofunctionalized Mt with the primary amine (ODA-Mt).

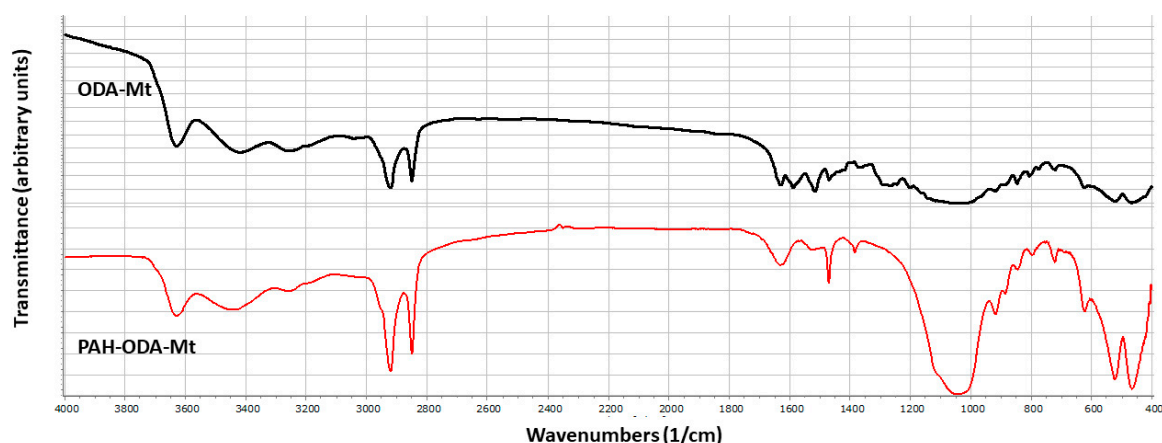


Figure 2. FT-IR transmittance spectra of ODA-Mt before and after adsorption assays in $4000\text{--}400\text{ cm}^{-1}$ region.

3.2. Characterization of Na-Mica-4, ODA-Mica-4 and ODTMA-Mica-4

3.2.1. X-ray Diffraction

XRD Le Bail adjustment for the Na-Mica-4, showed a GOF of 2.46 and residual factors Rwp of 11.96 and RBragg of 0.631. The structure used was Monoclinic, with P21 Spacegroup and lattice parameters as follows: a (Å) = 9.682(2), b (Å) = 5.2346(14), c (Å) = 12.032(3), β (°) = 91.356(9). For plane (001) d (Å) = 12.02889 and 2θ (°) = 7.34316 were obtained. For ODA-Mica-4 the Le Bail adjustment showed a GOF of 4.15 and residual factors Rwp of 17.96 and RBragg of 2.150. The structure used was Triclinic, with P1 Spacegroup and lattice parameters: a (Å) = 49.862(14), b (Å) = 9.992(3), c (Å) = 9.899(2), α (°) = 92.889(17), β (°) = 87.698(19), γ (°) = 89.500(18). For plane (001) d (Å) = 49.81865 and 2θ (°) = 1.77189 were obtained. For ODTMA-Mica-4 the Le Bail adjustment presented a GOF of 3.74 and residual factors Rwp of 11.97 and RBragg of 1.495. The structure used was Triclinic, with P1 Spacegroup and lattice parameters: a (Å) = 28.541(3), b (Å) = 10.0272(10), c (Å) = 10.0368(8), α (°) = 89.122(4), β (°) = 90.346(5), γ (°) = 88.479(4). For plane (001) d (Å) = 28.52992 and 2θ (°) = 3.09431 were obtained. Figure S3 presents the XRD diagrams for Na-Mica-4, ODA-Mica-4 and ODTMA-Mica-4.

The angle (α) of inclination of ODA and ODTMA axis in the interlayer space was 62.76° and 24.89° , respectively.

From the Le Bail fit, the mean crystallite domain size, D_{001} , obtained was 109(7) for Na-Mica-4, 157(11) for ODA-Mica-4 and 896(46) for ODTMA-Mica-4. The average number of clay platelets stacked (n) and calculated was 91.62 for Mt, 32.51 for ODA-Mt and 315.06 for ODTMA-Mt. The samples have high crystallite sizes and therefore a high stacking order, as can be seen in Figure S3.

3.2.2. Zeta Potential

The external surface charge of Na-Mica-4, ODA-Mica-4, and ODTMA-Mica-4 was studied at pH~6.5 and the obtained values were -28.4 , 39.5 , and 54.9 mV for Na-Mica-4, ODA-Mica-4, and ODTMA-Mica-4, respectively, before adsorption assays and 28.3 , 49.1 , and 45.8 mV for Na-Mica-4, ODA-Mica-4, and ODTMA-Mica-4, respectively, after adsorption assays.

3.2.3. Fourier-Transform Infrared Spectroscopy

Figure S4 shows the FT-IR spectra of Na-Mica-4, ODA-Mica-4, and ODTMA-Mica-4 in the $4000\text{--}400\text{ cm}^{-1}$ region. The characteristic bands of layered silicate and surfactants, already described in Section 3.1.3, can be appreciated. Figure 3 shows the vibrational spectra of ODA-Mica-4 before and after adsorption tests, without chemical transformation of the functional groups of the adsorbents [39,49,50]. As it was observed with the clay derived from Mt, the ODA-Mica-4 spectrum is where the PAH bands were most clearly observed.

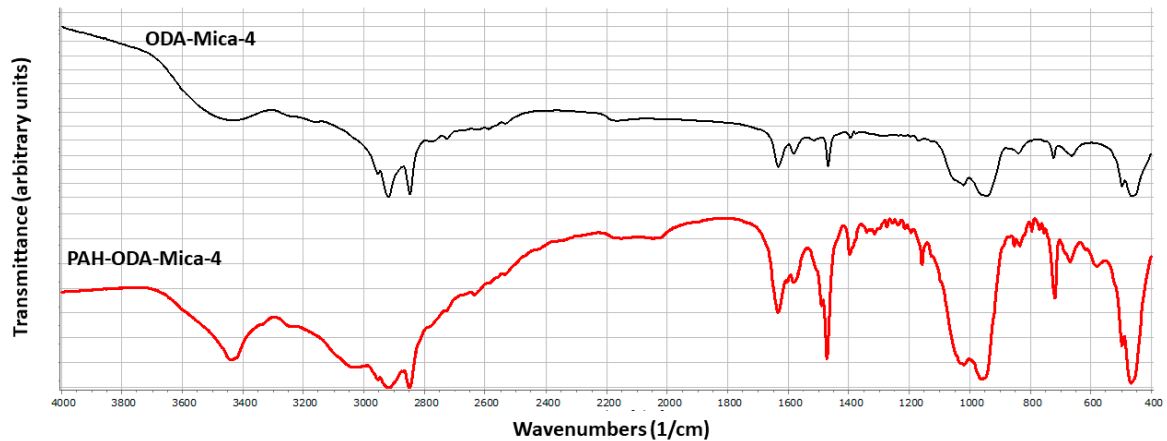


Figure 3. FT-IR transmittance spectra of ODA-Mica-4 before and after adsorption assays in $4000\text{--}400\text{ cm}^{-1}$ region.

3.3. Adsorption of PAHs

3.3.1. Adsorption onto Mt, ODA-Mt, and ODTMA-Mt

Figure 4A shows the adsorption % calculated for Mt and its organofunctionalized derivatives (ODA-Mt and ODTMA-Mt). Results were corroborated using both DAD and FI detectors. Overall, it can be observed that the adsorption of PAHs onto the Mt-based materials is very favorable, with adsorption percentage higher than 95%. When PAHs are put into contact with the aqueous solution, they are rapidly adsorbed onto the adsorbent materials mainly as a consequence of their hydrophobic property. Among the Mt-based materials, the optimal results were obtained with the pristine Mt adsorption rate of 100% for all PAHs. A slight decrease is observed when the Mt was organofunctionalized for some particular PAHs such as DahA (95%) in ODA-Mt or Ant (99%) in ODTMA-Mt. This fact leads us to think that the adsorption may occur both in the surface part and in the interlayer.

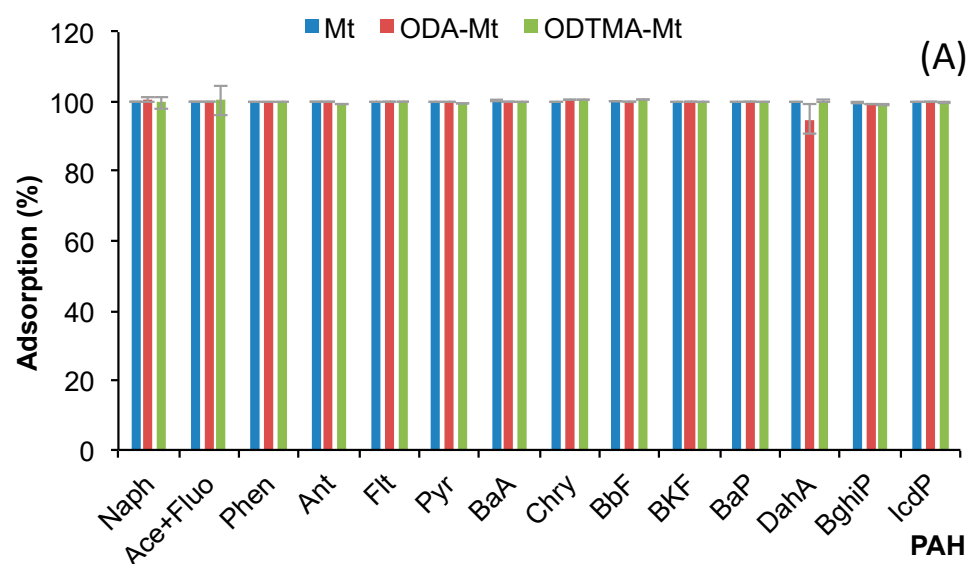


Figure 4. Cont.

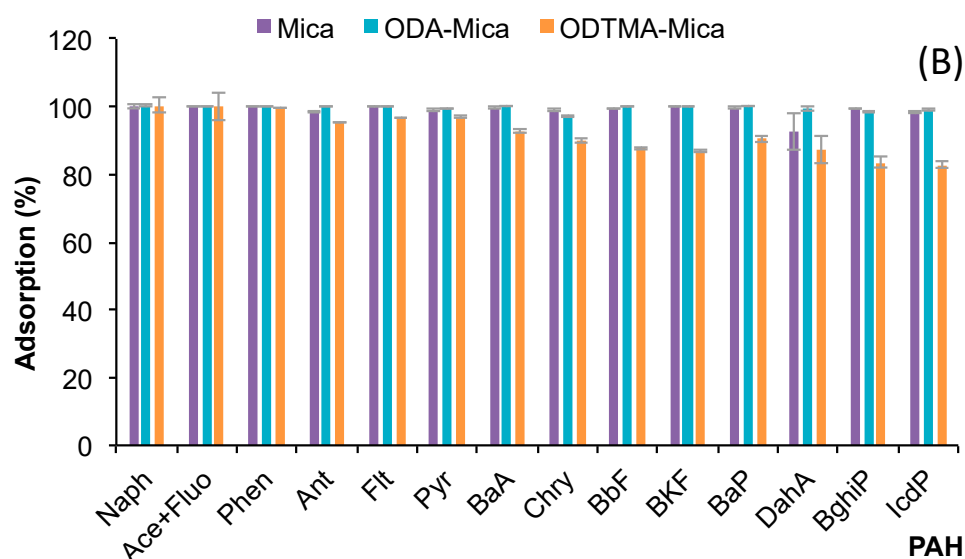


Figure 4. PAHs adsorption (%) on Mt and organofunctionalized derivatives (A) and Na-Mica-4 and organofunctionalized derivatives (B).

3.3.2. Adsorption onto Na-Mica-4, ODA-Mica-4, and ODTMA-Mica-4

Figure 4B shows the adsorption % for Na-Mica-4, ODA-Mica-4, and ODTMA-Mica-4. In comparison with Mt-based materials, the adsorption % was slightly lower for 12 out of 15 PAHs tested when Na-Mica-4 or organo-Na-Mica-4 clays were used. These results may be primarily explained by the higher surface area of Mt. Among the three Micas, the best adsorption % was observed for the unmodified Na-Mica-4. This fact was noticeably for BghiP (81% for ODTMA-Mica-4 vs. 100% for Na-Mica-4) and IcdP (84% for ODTMA-Mica-4 vs. 100% for Na-Mica-4).

4. Discussion

The synthesis of the Na-Mica-4 and the four organoclays through the ion exchange mechanism was successfully carried out. The diffractograms show an increase in the interlaminal spaces and the formation of a previously non-existent angle of inclination (α) between the aliphatic chains and the surface of the material after substituting the sodium ions for the alkylammonium and trialkylammonium chains. The measured Potential Z values agree with those assigned to previous works [36,47]. The IR-FT spectra show the signals corresponding to the characteristic functional groups of the 6 layered silicates [35,39,47,48] and reveals the presence of characteristic bands of PAH after adsorption assays [49,50], without appreciated changes in the signals of the characteristic groups of layered silicates, which would indicate the non-existence of chemical transformation of the materials.

Na-Mica-4, ODA-Mica-4, and ODTMA-Mica-4 present high crystallite sizes and therefore a high stacking order of the clay platelets. The three materials showed lower values of the stacking order, with the ODA-Mt being the most disordered case. This minor stacking order of the clay platelets can explain the greater effectiveness of Mt and its derivatives as there is a greater contact surface with PAHs.

The adsorption results showed that selected clay and modified clays are effective adsorbents of PAHs, with adsorption percentages very close to 100% (except for BghiP and IcdP, 81% and 84%, respectively). The adsorption of PAHs onto clay minerals is explained by the partition between nonpolar PAHs and the hydrophobic domain sites of clay minerals [51,52].

Among the two unmodified clays (Mt and Na-Mica-4), the one that presents the best percentages of PAH adsorption is the natural Mt which can be explained by its high surface area. Similar results were reported by Nanuam et al. [53]. The adsorption capability for BaP onto Mt was two times higher than onto kaolinite under a seawater solution, which is explained by the higher surface area of Mt as well as the effect of temperature.

Mt and Na-Mica-4 presented a better adsorption capacity than their organofunctionalized derivatives, which can indicate that the adsorption of PAHs may occur both in the surface part and in the interlayer of the clays. The presence of divalent cations such as Ca^{2+} and Mg^{2+} in unmodified materials such as Mt and Mica-4 can favor the retention of PAHs. In the presence of cations on the swelling clays, the π electron in the aromatic ring of PAHs builds the cation- π bonding. This bonding depends on (1) the π electron donation capacity of the aromatic ring present in the PAH and (2) the type of cations embedded on the clay surface [54]. According to Zhang et al. [52] due to these cations, PAHs can be further physically entrapped through capillary condensation in the nano- and micropores due to the formation of PAH quasicrystals via strong cross-linking bonds.

According to literature studies, clays have proven to be effective materials to remove PAHs from aqueous solutions. Nkansa et al. [55] used a lightweight expanded clay aggregate as sorbent for PAHs removal from water. The adsorption % was higher than 70% for Phen, Flt, and Pyr when a mass of 0.2 g of sorbent was used, although an increase in the adsorption capability up to 94% was observed when 4.0 g of the lightweight expanded clay aggregate was used. In another attempt, the adsorption capacity for PAHs onto the organo-Mt-Alginate bionanocomposite was ordered as follows: Phe (2.50 mg/g) > Ace (1.20 mg/g) > Flu (0.90 mg/g), which is in agreement with the degree of hydrophobicity of selected PAHs. Wiles et al. [56] revealed that Naph, Fluo, Phen, Pyr, and total PAHs can be >99%, 61%, 99%, 99%, 97%, and 94% removed, respectively, using the combination cetyl-pyridinium-Mt/active carbon from water samples.

Regarding soil samples, its physicochemical properties determine the processes occurring inside, including the degradation and accumulation of pollutants of anthropogenic origin. It is generally accepted that the sorption of PAHs plays a key role in their movement and determines the bioavailability. Studies have revealed the positive impact of the mineral fraction of soils on sorption to retain PAHs [51,57]. The sorption properties of minerals depend on their crystal structure. In this sense, the most important mineral group is clay minerals. Justyna et al. [57] revealed that the increase in both clay fraction and the humic acids resulted in an increase in the sorption of Phen onto soil. Moreover, Mt showed higher sorption (removal efficiency > 99%) than humic acids. Due to the immobilization of xenobiotics, these kind of soils, are less likely to transfer contamination into agricultural products. In another attempt, Hundal et al. [51] indicated that soil containing smectite can retain a large amount of Phen.

Although over the last years an increasing number of studies focusing on clays as adsorbent materials of a large variety of organic and inorganic pollutants have been conducted, at this stage, the focus tends to be limited to the laboratory scale [15,20,24–26]. In a near future more work needs to be performed to bridge the knowledge gap in evaluating the efficiencies of clays and modified clays in treating real wastewater effluent or soil samples. To the best of our knowledge, a full-scale application has not yet been demonstrated in any remediation site or water treatment.

5. Conclusions

In this study, six different clay materials, the natural Mt and the synthetic Na-Mica-4 and four organomodified of the last ones with octadecylamine (ODA-Mt and ODA-Mica-4) and octadecyltrimethylamine (ODTMA-Mt and ODTMA-Mica-4) were prepared and compared for the adsorption of PAHs for the first time.

This study demonstrates the high affinity of certain clays for PAHs, and therefore opens a line of research of materials that can deal with activated carbon as an ecological alternative in its use for wastewater treatment and soil remediation to prevent PAH pollution.

Supplementary Materials: The following are available online at <https://www.mdpi.com/article/10.3390/environments8110124/s1>, Figure S1: XRD results for the 001 reflections of the samples Mt (black line), ODA-Mt (red line) and ODTMA-Mt (blue line), Figure S2: FT-IR transmittance spectra of Mt, ODA-Mt and ODTMA-Mt in 4000–400 cm⁻¹ region, Figure S3: XRD results for the samples Na-Mica-4 (black line), ODA-Mica-4 (red line) and ODTMA-Mica-4 (blue line), Figure S4: FT-IR transmittance spectra of Na-Mica-4, ODA-Mica-4 and ODTMA-Mica-4 in 4000–400 cm⁻¹ region.

Author Contributions: Investigation and Validation, S.S.; Conceptualization, Supervision, Writing—review and editing, J.M. and M.d.M.O.; Formal analysis, Methodology and Writing—review and editing, S.M.-C.; Conceptualization, N.M. and N.B.; Conceptualization, Methodology and Formal analysis, J.L.S.; Conceptualization and Supervision, I.A.; Project administration and Funding acquisition, E.A. All authors have read and agreed to the published version of the manuscript.

Funding: This research was funded by the Spanish Ministry of Economy, Industry and Competitiveness (Project No. CTM2017-82778-R).

Institutional Review Board Statement: Not applicable.

Informed Consent Statement: Not applicable.

Data Availability Statement: Not applicable.

Conflicts of Interest: The authors declare no conflict of interest.

References

1. Hedayati, M.S.; Abida, O.; Li, L.Y. Adsorption of polycyclic aromatic hydrocarbons by surfactant-modified clinoptilolites for landfill leachate treatment. *Waste Manag.* **2021**, *131*, 503–512. [[CrossRef](#)] [[PubMed](#)]
2. Balati, A.; Shahbazi, A.; Amini, M.M.; Hashemi, S.H. Adsorption of polycyclic aromatic hydrocarbons from wastewater by using silica-based organic-inorganic nanohybrid material. *J. Water Reuse Desalination.* **2015**, *5*, 50. [[CrossRef](#)]
3. Vane, C.H.; Kim, A.W.; Beriro, D.J.; Cave, M.R.; Knights, K.; Moss-Hayes, V.; Nathanail, P.C. Polycyclic aromatic hydrocarbons (PAH) and polychlorinated biphenyls (PCB) in urban soils of Greater London, UK. *Appl. Geochem.* **2014**, *51*, 303–314. [[CrossRef](#)]
4. Wang, J.; Wang, C.; Huang, Q.; Ding, F.; He, X. Adsorption of PAHs on the sediments from the yellow river delta as a function of particle size and Salinity. *Soil Sediment. Contam. Int. J.* **2015**, *24*, 103–115. [[CrossRef](#)]
5. Liu, Y.; Gao, Y.; Yu, N.; Zhang, C.; Wang, S.; Ma, L.; Zhao, J.; Lohmann, R. Particulate matter, gaseous and particulate polycyclic aromatic hydrocarbons (PAHs) in an urban traffic tunnel of China: Emission from on-road vehicles and gas-particle partitioning. *Chemosphere* **2015**, *134*, 52–59. [[CrossRef](#)]
6. USEPA. *Polycyclic Aromatic Hydrocarbons (Pahs) Fact Sheet*; National Center for Environmental Assessment, Office of Research and Development: Washington, DC, USA, 2008.
7. Manoli, E.; Samara, C. Polycyclic aromatic hydrocarbons in natural waters: Sources, occurrence and analysis. *Tr. Anal. Chem.* **1999**, *18*, 417–428. [[CrossRef](#)]
8. Siddens, L.K.; Larkin, A.; Krueger, S.K.; Bradfield, C.A.; Waters, K.M.; Tilton, S.C.; Pereira, C.B.; Lohr, C.V.; Arlt, V.M.; Phillips, D.H.; et al. Polycyclic aromatic hydrocarbons as skin carcinogens: Comparison of benzo[a]pyrene, dibenzo[def,p]chrysene and three environmental mixtures in the FVB/N mouse. *Toxicol. Appl. Pharmacol.* **2012**, *264*, 377–386. [[CrossRef](#)]
9. Xu, X.H.; Hu, H.; Kearney, G.D.; Kan, H.D.; Sheps, D.S. Studying the effects of polycyclic aromatic hydrocarbons on peripheral arterial disease in the United States. *Sci. Total Environ.* **2013**, *461*, 341–347. [[CrossRef](#)]
10. Chen, B.L.; Zhou, D.D.; Zhu, L.Z. Transitional adsorption and partition of nonpolar and polar aromatic contaminants by biochars of pine needles with different pyrolytic temperatures. *Environ. Sci. Technol.* **2008**, *42*, 5137–5143. [[CrossRef](#)]
11. Makkar, R.S.; Rockne, K.J. Comparison of synthetic surfactants and biosurfactants in enhancing biodegradation of polycyclic aromatic hydrocarbons. *Environ. Toxicol. Chem.* **2003**, *22*, 2280–2292. [[CrossRef](#)]
12. Chomanee, J.; Tekasakul, S.; Tekasakul, P.; Furuuchi, M. Effect of irradiation energy and residence time on decomposition efficiency of polycyclic aromatic hydrocarbons (PAHs) from rubber wood combustion emission using soft X-rays. *Chemosphere* **2018**, *210*, 417–423. [[CrossRef](#)] [[PubMed](#)]
13. Boulange, M.; Lorgeoux, C.; Biache, C.; Saada, A.; Faure, P. Fenton-like and potassium permanganate oxidations of PAH-contaminated soils: Impact of oxidant doses on PAH and polar PAC (polycyclic aromatic compound) behaviour. *Chemosphere* **2019**, *224*, 437–444. [[CrossRef](#)] [[PubMed](#)]
14. Anna, K.I.; Emanuel, G.; Anna, S.R.; Blonska, E.; Lasota, J.; Lagan, S. Linking the contents of hydrophobic PAHs with the canopy water storage capacity of coniferous trees. *Environ. Pollut.* **2018**, *242*, 1176–1184. [[CrossRef](#)] [[PubMed](#)]
15. Sabah, E.; Ouki, S. Adsorption of pyrene from aqueous solutions onto sepiolite. *Clays Clay Miner.* **2017**, *65*, 14–26. [[CrossRef](#)]
16. Lamichhane, S.; Bal Krishna, K.C.; Sarukkalghe, R. Polycyclic aromatic hydrocarbons (PAHs) removal by sorption: A review. *Chemosphere* **2016**, *148*, 336–353. [[CrossRef](#)] [[PubMed](#)]
17. Awad, A.M.; Shaikh, S.M.R.; Jalab, R.; Gulied, M.H.; Nasser, M.S.; Benamor, A.; Adham, S. Adsorption of organic pollutants by natural modified clays: A comprehensive review. *Sep. Purif. Technol.* **2019**, *228*, 115719. [[CrossRef](#)]

18. Lemi, J.; Tomasevi-Canovi, M.; Adamovi, M.; Kovacevi, D.; Milicevi, S. Competitive adsorption of polycyclic aromatic hydrocarbons on organo-zeolites. *Microporous Mesoporous Mater.* **2007**, *105*, 317–323. [[CrossRef](#)]
19. Mukherjee, S. Clays as neutralizers against environmental protection. In *The Science of Clays*; Mukherjee, S., Ed.; Springer: Dordrecht, The Netherlands, 2013; pp. 250–263.
20. González-Santamaría, D.E.; López, E.; Ruiz, A.; Ortega, A.; Cuevas, J. Adsorption of phenanthrene by stevensite and sepiolite. *Clay Min.* **2017**, *52*, 341–350. [[CrossRef](#)]
21. Bergaya, F.; Lagaly, G. (Eds.) Introduction on modified clays and clay minerals. In *Developments in Clay Science*; Elsevier: Amsterdam, The Netherlands, 2013; pp. 383–557.
22. Sarkar, B.; Xi, Y.F.; Megharaj, M.; Krishnamurti, G.S.R.; Bowman, M.; Rose, H.; Naidu, R. Bioreactive organoclay: A new technology for environmental remediation. *Crit. Rev. Environ. Sci. Technol.* **2012**, *42*, 435–488. [[CrossRef](#)]
23. Churchman, G.J.; Gates, W.P.; Theng, B.K.G.; Yuan, G. Clays and clay minerals for pollution control. In *Developments in Clay Science*; Bergaya, F., Theng, B.K.G., Lagaly, G., Eds.; Elsevier: Amsterdam, The Netherlands, 2006; pp. 625–675.
24. Orta, M.M.; Martín, J.; Medina-Carrasco, S.; Santos, J.L.; Aparicio, I.; Alonso, E. Novel synthetic clays for the adsorption of surfactants from aqueous media. *J. Environ. Manag.* **2018**, *206*, 357–363. [[CrossRef](#)]
25. Martín, J.; Orta, M.M.; Medina-Carrasco, S.; Santos, J.L.; Aparicio, I.; Alonso, E. Removal of priority and emerging pollutants from aqueous media by adsorption onto synthetic organofunctionalized high-charge swelling micas. *Environ. Res.* **2018**, *164*, 488–494. [[CrossRef](#)] [[PubMed](#)]
26. Dai, W.-J.; Wu, P.; Liu, D.; Hu, J.; Cao, Y.; Liu, T.-Z.; Okoli, C.P.; Wang, B.; Li, L. Adsorption of polycyclic aromatic hydrocarbons from aqueous solution by organic montmorillonite sodium alginate nanocomposites. *Chemosphere* **2020**, *251*, 126074. [[CrossRef](#)] [[PubMed](#)]
27. Li, F.; Chen, J.; Hu, X.; He, F.; Bean, E.; Tsang, D.C.W.; Ok, Y.S.; Gao, B. Applications of carbonaceous adsorbents in the remediation of polycyclic aromatic hydrocarbon-contaminated sediments: A review. *J. Clean. Prod.* **2020**, *255*, 120263. [[CrossRef](#)]
28. Funada, M.; Nakano, T.; Moriwaki, H. Removal of polycyclic aromatic hydrocarbons from soil using a composite material containing iron and activated carbon in the freeze-dried calcium alginate matrix: Novel soil cleanup technique. *J. Hazard. Mat.* **2018**, *351*, 232–239. [[CrossRef](#)]
29. Kumar, M.; Bolan, N.S.; Hoang, S.A.; Sawarkar, A.D.; Jasemizad, T.; Gao, B.; Keerthanan, S.; Padhye, L.P.; Singh, L.; Kumar, S.; et al. Remediation of soils and sediments polluted with polycyclic aromatic hydrocarbons: To immobilize, mobilize, or degrade? *J. Hazard. Mat.* **2021**, *420*, 126534. [[CrossRef](#)]
30. Samuelsson, G.S.; Hedman, J.E.; Kruså, M.E.; Gunnarsson, J.S.; Cornelissen, G. Capping in situ with activated carbon in Trondheim harbor (Norway) reduces bioaccumulation of PCBs and PAHs in marine sediment fauna. *Mar. Environ. Res.* **2015**, *109*, 103–112. [[CrossRef](#)]
31. International Programme on Chemical Safety (Ed.) Selected non-heterocyclic polycyclic aromatic hydrocarbons. In *Environmental Health Criteria*; World Health Organization: Geneva, Switzerland, 1998.
32. Magnoli, A.P.; Tallone, L.; Rosa, C.A.R.; Dalcero, A.M.; Chiacchiera, S.M.; Torres Sanchez, R.M. Commercial bentonites as detoxifier of broiler feed contaminated with aflatoxin. *Appl. Clay Sci.* **2008**, *40*, 63–71. [[CrossRef](#)]
33. Gamba, M.; Flores, F.M.; Madejová, J.; Sánchez, R.M.T. Comparison of imazalil removal onto montmorillonite and nanomontmorillonite and adsorption surface sites involved: An approach for agricultural wastewater treatment. *Ind. Eng. Chem. Res.* **2015**, *54*, 1529–1538. [[CrossRef](#)]
34. Alba, M.D.; Castro, M.A.; Naranjo, M.; Pavón, E. Hydrothermal Reactivity of Na-n-Micas (n = 2, 3, 4). *Chem. Mat.* **2006**, *18*, 2867–2872. [[CrossRef](#)]
35. Flores, F.M.; Loveira, E.L.; Yarza, F.; Candal, R.; Sánchez, R.M.T. Benzalkonium chloride surface adsorption and release by two montmorillonites and their modified organomontmorillonites. *Water Air Soil Poll* **2017**, *28*, 42. [[CrossRef](#)]
36. Orta, M.M.; Flores, F.M.; Fernández Morantes, C.; Curutchet, G.A.; Torres Sanchez, R.M. Interrelations of structure, electric surface charge, and hydrophobicity of organomica and montmorillonite, tailored with quaternary or primary amine cations. Preliminary study of pyrimethanil adsorption. *Mat. Chem. Phys.* **2019**, *223*, 325–335. [[CrossRef](#)]
37. Bruker, A.X.S. *TOPAS 6 User Manual*; Bruker: Billerica, MA, USA, 2017.
38. Le Bail, A. Whole powder pattern decomposition methods and applications: A retrospection. *Powder Diff.* **2005**, *20*, 316. [[CrossRef](#)]
39. Alba, M.D.; Castro, M.A.; Orta, M.M.; Pavón, E.; Pazos, M.C.; Valencia Rios, J.S. Formation of organo-highly charged mica. *Langmuir* **2011**, *27*, 9711–9718. [[CrossRef](#)]
40. Solarte, A.L.F.; Villarroel-Rocha, J.; Morantes, C.F.; Montes, M.L.; Sapag, K.; Curutchet, G.; Sánchez, R.M.T. Insight into surface and structural changes of montmorillonite and organomontmorillonites loaded with Ag. *Comptes Rendus Chim.* **2019**, *22*, 142–153. [[CrossRef](#)]
41. Huang, P.; Kazlauciuonas, A.; Menzel, R.; Lin, L. Determining the mechanism and efficiency of industrial dye adsorption through facile structural control of organomontmorillonite adsorbents. *ACS Appl. Mater. Interfaces* **2017**, *9*, 26383–26391. [[CrossRef](#)]
42. Smoluchowski, R. Anisotropy of the electronic work function of metals. *Phys. Rev.* **1941**, *60*, 661–674. [[CrossRef](#)]
43. Wang, C.; Zhou, S.; Wu, S.; Song, J.; Shi, Y.; Li, B.; Chen, H. Surface water polycyclic aromatic hydrocarbons (PAH) in urban areas of Nanjing, China. *Water Sci. Technol.* **2017**, *76*, 2150–2157. [[CrossRef](#)]
44. Kalmykova, Y.; Moona, N.; Strömvall, A.M.; Björklund, K. Sorption and degradation of petroleum hydrocarbons, polycyclic aromatic hydrocarbons, alkylphenols, bisphenol A and phthalates in landfill leachate using sand, activated carbon and peatfilters. *Water Res.* **2014**, *56*, 246–257. [[CrossRef](#)]
45. Björklund, K.; Li, L. Evaluation of low-cost materials for sorption of hydrophobic organic pollutants in stormwater. *J. Environ. Manag.* **2015**, *159*, 106–114. [[CrossRef](#)]

46. Santos, J.L.; Aparicio, I.; Alonso, E. A new method for the routine analysis of LAS and PAH in sewage sludge by simultaneous sonication-assisted extraction prior to liquid chromatographic determination. *Anal. Chim. Acta* **2007**, *605*, 102–109. [[CrossRef](#)]
47. Malvar, J.L.; Martín, J.; Orta, M.M.; Medina-Carrasco, S.; Santos, J.L.; Aparicio, I.; Alonso, E. Simultaneous and individual adsorption of ibuprofen metabolites by a modified montmorillonite. *Appl. Clay Sci.* **2020**, *189*, 105529. [[CrossRef](#)]
48. Scheuing, D.R. (Ed.) *Fourier Infrared Spectroscopy in Colloid and Interface Science*; ACS Symposium Series 447; American Chemical Society: Washington, DC, USA, 1990; pp. 1–21.
49. Hudgins, D.M.; Sandford, S.A. Infrared spectroscopy of matrix isolated polycyclic aromatic hydrocarbons. PAHs containing two to four rings. *J. Phys. Chem. A* **1998**, *102*, 329–343. [[CrossRef](#)]
50. Sandford, S.A.; Bernstein, M.P.; Materese, C.K. The infrared spectra of polycyclic aromatic hydrocarbons with excess peripheral H atoms (Hn-PAHs) and their relation to the 3.4 and 6.9 μm PAH emission features. *Astrophys. J. Suppl. Ser.* **2013**, *205*, 8. [[CrossRef](#)] [[PubMed](#)]
51. Hundal, L.S.; Thompson, M.L.; Laird, D.A.; Carmo, A.M. Sorption of phenanthrene by reference smectites. *Environ. Sci. Technol.* **2001**, *35*, 3456–3461. [[CrossRef](#)]
52. Zhang, W.; Zhuang, L.; Yuan, Y.; Tong, L.; Tsang, D.C.W. Enhancement of phenanthrene adsorption on a clayey soil and clay minerals by coexisting lead or cadmium. *Chemosphere* **2011**, *83*, 302–310. [[CrossRef](#)]
53. Nanuam, J.; Zuddas, P.; Sawangwong, P.; Pachana, K. Modeling of PAHs adsorption on Thai clay minerals under seawater solution conditions. *Procedia Earth Planet. Sci.* **2013**, *607–610*, 1878–5220.
54. Biswas, B.; Sarkar, B.; Rusmin, R.; Naidu, R. Bioremediation of PAHs and VOCs: Advances in clay mineral–microbial interaction. *Environ. Int.* **2015**, *85*, 168–181. [[CrossRef](#)]
55. Nkansah, M.A.; Christy, A.A.; Barthb, T.; Francis, G.W. The use of lightweight expanded clay aggregate (LECA) as sorbent for PAHs removal from water. *J. Hazard Mat.* **2012**, *217–218*, 360–365. [[CrossRef](#)]
56. Wiles, M.C.; Huebner, H.J.; McDonald, T.J.; Donnelly, K.C.; Phillips, T.D. Matrix immobilized organoclay for the sorption of polycyclic aromatic hydrocarbons and pentachlorophenol from groundwater. *Chemosphere* **2005**, *59*, 1455–1464. [[CrossRef](#)]
57. Justyna, S.; Zuzanna, S.; Paweł, C.; Agnieszka, P. The effect of organic and clay fraction on polycyclic aromatic hydrocarbons mobility in soil model systems. *J. Res. Appl. Agric. Eng.* **2015**, *60*, 98–101.